

Supramolecular aggregates between carboxylate anions and an octaaza macrocyclic receptor

Carla Cruz,^{a,b} Rita Delgado,^{*b,c} Michael G. B. Drew^d and Vítor Félix^{*a}

^a Departamento Química, CICECO, Universidade de Aveiro, 3810-193 Aveiro, Portugal. E-mail: vfelix@dq.ua.pt

^b Instituto de Tecnologia Química e Biológica, UNL, Apartado 127, 2781-901, Oeiras, Portugal. E-mail: delgado@itqb.unl.pt

^c Instituto Superior Técnico, Av. Rovisco Pais, 1049-001 Lisboa, Portugal

^d School of Chemistry, University of Reading, Whiteknights, Reading, UK RG6 6AD

Received 4th August 2004, Accepted 9th August 2004

First published as an Advance Article on the web 14th September 2004

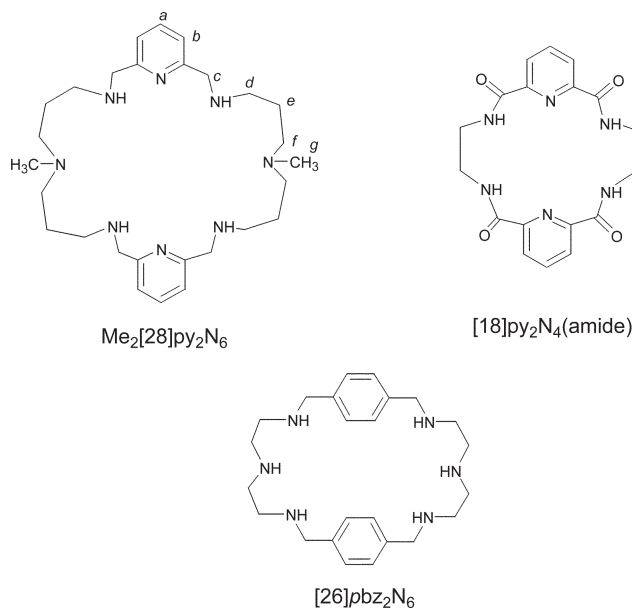
The 28-membered octaazamacrocyclic receptor $\text{Me}_2[28]\text{py}_2\text{N}_6$ was used as a receptor for the molecular recognition of aromatic and aliphatic carboxylate substrates. The receptor-substrate binding behaviour of $(\text{H}_6\text{Me}_2[28]\text{py}_2\text{N}_6)^{6+}$ with an aliphatic ($^-\text{O}_2\text{C}(\text{CH}_2)_n\text{CO}_2^-$, $n = 0$ to 4) and an aromatic (phthalate, isophthalate, terephthalate, 4,4'-dibenzoate, benzoate, 3- and 4-nitrobenzoate) series of carboxylate anions was evaluated by ^1H NMR spectroscopy (carried out in $\text{DMSO}-d_6$ at 300 K). Two association constants were found for most of the studied cases, except for 3- and 4-nitrobenzoate for which only K_1 was determined. For oxalate, malonate, benzoate and dibenzoate anions only the β_2 constants could be obtained. The values of the first association constant cover a range from 2.86 to 3.69 (log units), and the second stepwise constant from 2.15 to 2.89 (also in log units). No special selectivity was found but the highest values were determined for adipate and the lowest for the monoprotic 3- and 4-nitrobenzoates. Single crystal X-ray structures of $\text{H}_6\text{Me}_2[28]\text{py}_2\text{N}_6^{6+}$ with terephthalate, **1**, and 4,4'-dibenzoate (**2**) were determined showing supramolecular entities with general formula $(\text{H}_6\text{Me}_2[28]\text{py}_2\text{N}_6) \cdot (\text{substrate})_2(\text{PF}_6)_2 \cdot 4\text{H}_2\text{O}$. These anions are the building blocks of an extensive 3-D network of hydrogen bonds.

Introduction

Anion recognition by synthetic receptors has been one of the most rapidly growing chemical research fields in the last decade. Indeed, anions play essential roles in chemical as well as in biological processes, encouraging the development of novel synthetic receptors displaying anion selectivity.¹⁻⁶ The recognition of anionic substrates requires complementary positively charged or electron-deficient sites to form electrostatic, hydrophobic and/or hydrogen bonding interactions. Other weak interactions, such as π - π stacking, cation- π or *van der Waals*, can cooperatively contribute to the molecular selective recognition phenomena.

Among the anions, carboxylates are an important functional group in organic and biological molecules which give rise to a wide range of synthetic receptors.³ The most common complementary sites for carboxylate anions are ammonium (quaternary salts or protonated polyamines), amidinium, guanidinium, amides, urea or thiourea centres or Lewis acids.¹⁻⁶ Lehn *et al.* were the pioneers in determining association constants for polyammonium macrocycles with a set of carboxylate anions in water,⁷ followed by Kimura *et al.*⁸ Most of the studies in this field have been carried out in solution. By contrast, there are few X-ray structural determinations of supermolecules with inclusion of anions. The majority of the reported structures have halide or oxoanions (NO_3^- , SO_4^{2-} , HPO_4^{2-} , and others) as substrates, while supermolecules including linear bifunctional anions are scarce.⁹ Three types of receptors are currently found in X-ray determinations of these associations: macrocycles,¹⁰⁻¹³ calixarenes,¹⁴ cryptands,¹⁵⁻¹⁸ and linear receptors having special functionalities, such as cyclic guanidinium,^{19,20} and amide.²¹⁻²² In only a few cases is the substrate completely encapsulated by the receptor. Among the most suitable architectures for the inclusion of substrates, the cryptands offer appropriate 3-dimensional cages to encapsulate terephthalate,¹⁵ acetate,¹⁶ or oxalate^{17,18} anions. Macrocycles are also able to accommodate anions as found in the supermolecule formed by a 26-membered hexaazamacrocyclic (see Scheme 1) and the oxalate anion, recently reported by Llobet *et al.*¹³ Alternatively, the anion threads through the macrocyclic framework, forming a 1:1 associated

species, such as occurs with oxalate and a hexaazamacrocyclic having two furan spacers.¹¹ Finally, the molecular recognition phenomena between the macrocycle and the anion substrate can occur outside the macrocyclic cavity giving rise to supramolecular entities with stoichiometries different from 1:1. For example, the acetate bridges two $[18]\text{py}_2\text{N}_4$ (amide) (see Scheme 1) derivative in a 2:1 R:S sandwich complex (R is used to designate the receptor and S the substrate).¹⁰



Scheme 1

In several other cases the anion substrates bind the macrocyclic receptors *via* an extensive 3-D network of hydrogen-bonds,⁴ as is found with the 28-membered hexaazamacrocyclic ($\text{H}_6\text{Me}_2[28]\text{py}_2\text{N}_6^{6+}$) which is assembled by oxydiacetate anions vertically located above and below the cavity.¹³

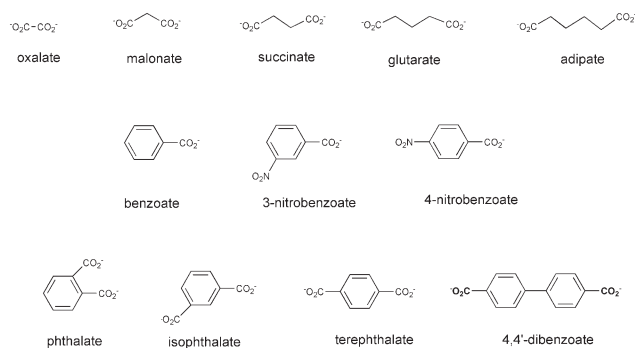
In order to gain further insights into the features that control the inclusion of linear substrates, we report in this

Table 1 ^1H NMR resonances (δ ppm) and shifts ($\Delta\delta = \delta_{\text{obs}} - \delta_{\text{R}}$) for H_c , H_f and H_g protons of the protonated macrocycle (R) upon addition of the substrate on saturation

Substrate ^a	H_c		H_f		H_g	
	δ	$\Delta\delta$	δ	$\Delta\delta$	δ	$\Delta\delta$
Oxalate	4.301	0.150	2.525	0.610	2.195	0.640
Malonate	4.331	0.120	2.655	0.480	2.339	0.496
Succinate	3.968	0.483	2.395	0.740	2.155	0.680
Glutarate	3.778	0.673	2.331	0.804	2.124	0.711
Adipate	3.741	0.710	2.308	0.827	2.105	0.730
Benzoate	3.881	0.570	2.419	0.716	2.136	0.699
3-Nitrobenzoate	4.290	0.161	2.805	0.330	2.522	0.313
4-Nitrobenzoate	4.241	0.210	2.819	0.316	2.526	0.309
Phthalate	4.206	0.245	2.536	0.599	2.227	0.608
Isophthalate	4.171	0.280	2.515	0.620	2.255	0.580
Terephthalate	3.981	0.470	2.415	0.720	2.445	0.390
4,4'-Dibenzoate	3.889	0.562	2.691	0.444	2.418	0.417

^aThe resonances found for the receptor $\text{H}_6\text{Me}_2[28]\text{py}_2\text{N}_6^{6+}$ are: 4.451 (H_c), 3.135 (H_f) and 2.835 (H_g).

work the association of the macrocycle 7,23-dimethyl-3,7,11,19,23,27,33,34-octaazatricyclo[27.3.1.1^{13,17}]tetra-triacontane-1(32),13(14),15,17, 29,31-hexaene ($\text{Me}_2[28]\text{py}_2\text{N}_6$) with two sets of carboxylate anions differing in shape, size and rigidity: an aliphatic (oxalate, malonate, succinate, glutarate and adipate), and an aromatic series (phthalate, isophthalate, terephthalate, and 4,4'-dibenzoate). For comparison purposes three monocarboxylate anions were also studied: namely benzoate, 3- and 4-nitrobenzoate anions (see Scheme 2).



Scheme 2

Results and discussion

Binding affinities in solution: ^1H NMR titrations

All the secondary amines of the ligand $\text{Me}_2[28]\text{py}_2\text{N}_6$ are fully protonated at pH 5 ($\log K_1 = 9.87$, $\log K_2 = 9.18$, $\log K_3 = 8.30$, $\log K_4 = 7.63$, $\log K_5 = 6.83$, $\log K_6 = 6.32$, $\log K_7 = 3.21$, $\log K_8 = 2.81$, $\log \beta_8 = 48.13$)²³ forming a highly charged polyammonium cation in solution, $\text{H}_6\text{Me}_2[28]\text{py}_2\text{N}_6^{6+}$ (R), which can interact with anions by electrostatic and hydrogen bonding interactions.

For solubility reasons the experiments for the determination of the association constants were carried out in DMSO. Due to the high solvating tendency of this solvent, affinities to anions will be lower compared to those found in non-polar solvents. For the same reason, anionic substrates were studied as their tetramethylammonium salts. However, the potassium salt of oxalate has enough solubility to allow experiments to be carried out, which showed that changing the counterion (K^+ versus Me_4N^+) did not affect the strength of the binding interaction.

Two series of carboxylate anions were studied. The first one is a series of aliphatic and flexible dicarboxylate anions with increasing number of methylenic carbons between the two terminal carboxylate groups. The second series includes rigid aromatic substrates with the two carboxylate groups located at different positions of a benzene ring, *ortho*-, *meta*- and *para*- (phthalate, isophthalate and terephthalate, respectively), and 4,4'-dibenzoate. The presence of the aromatic ring allows studies of the effects of the increase in rigidity of the substrate

as well as the potential π - π stacking interactions between the aromatic rings of the substrate and the receptor.

^1H NMR was used to follow the values of $\Delta\delta = (\delta_{\text{obs}} - \delta_{\text{R}})$ by addition of known amounts of anion solutions. Separated ^1H NMR signals were found for the receptor and the substrate protons upon formation of the receptor-substrate entity, indicating a fast exchange between the free receptor and complex compared to the NMR time scale. All the resonances of the free receptor shift highfield, including the protons of the pyridine ring, suggesting that the ammonium donor atoms of the receptor are involved in interactions with the anions, which can be accomplished by conformational changes. Two types of patterns were observed for the different resonances. Resonances H_a , H_b , H_c and H_d have small shifts of $\Delta\delta$ during the addition of the first two equivalents of anion solutions and then have sharper shifts, whereas H_f and H_g have the opposite behaviour, with a sharp change during the addition of the first two equivalents of anions and a small change after that value. Protons H_c , due to their specific position in the receptor molecule, present an intermediate pattern. The typical shifts found for three resonances H_c , H_f and H_g in the protonated macrocycle upon addition of the different substrates on saturation are listed in Table 1, while in Fig. 1 the H_c and H_g proton shifts along the titration are shown. These titration profiles indicate that the carboxylate group of the first equivalents of anions added interacts directly with the central ammonium ion of the receptor, HNCH_3^+ , and in a second stage the interaction proceeds with ammonium groups contiguous to the pyridine rings. Job's plots^{24,25} performed for the titrations with malonate, glutarate and terephthalate, showed that two species are formed in solution, R:S and R:2S. Job's plots for the terephthalate anion are shown in Fig. 2 as a function of the receptor and substrate, respectively.

Association constants were determined from ^1H NMR titration curves with the program HypNMR,²⁶ using the maximum number of possible resonances. The calculated values for all the anions are collected in Table 2. Most of the systems converged for two constants, corresponding to RS and RS_2 species, as also indicated by Job's plots (see Fig. 2); the exceptions being the monocarboxylate anions 3- and 4-nitrobenzoate, for which only K_1 was found. On the other hand, for oxalate, malonate, benzoate and 4,4'-dibenzoate only the overall constant (β_2 constant) corresponding to the formation of RS_2 was determined.

The values of association constants reveal relatively strong binding for the first substrate and slightly weaker binding for the second. However, no perceptible selectivity was observed for this series of anions, although the association with isophthalate and adipate shows the highest K_1 and the latter substrate exhibits also the highest β_2 value. The smallest K_1 values were found for 3- and 4-nitrobenzoate.

The values of K_2 are lower than K_1 , but both values do not differ too much, suggesting that they correspond to the same

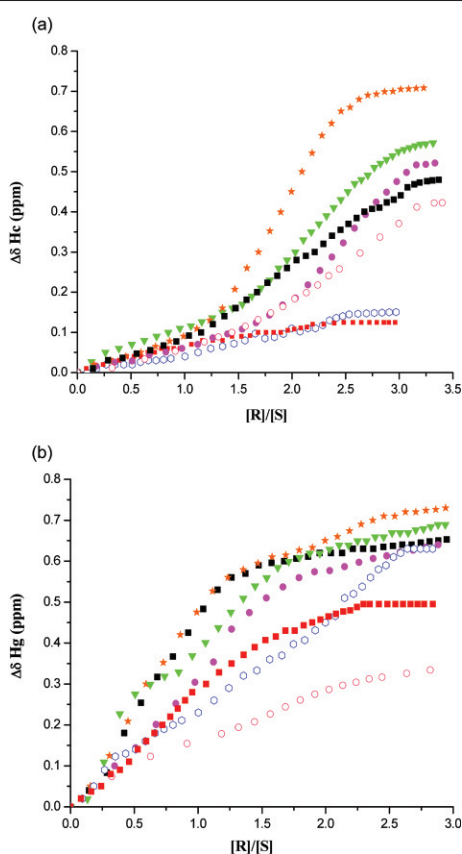


Fig. 1 ^1H NMR titration of $(\text{H}_6\text{Me}_2[28]\text{py}_2\text{N}_6)(\text{PF}_6)_6$ with several anions, $\Delta\delta$ of the protons of the receptor in function of the number of equivalents of substrate added, in $\text{DMSO}-d_6$ (a) following the singlet H_c , and (b) the singlet of the $^+\text{NCH}_3$ (H_d) of the receptor. The symbols of the anions are: oxalate (\circ , blue), malonate (\blacksquare , red), succinate (\blacksquare , black), glutarate (\bullet , purple), adipate (\star , orange), benzoate (\blacktriangledown , green), and 4,4'-dibenzoate (\circ , pink).

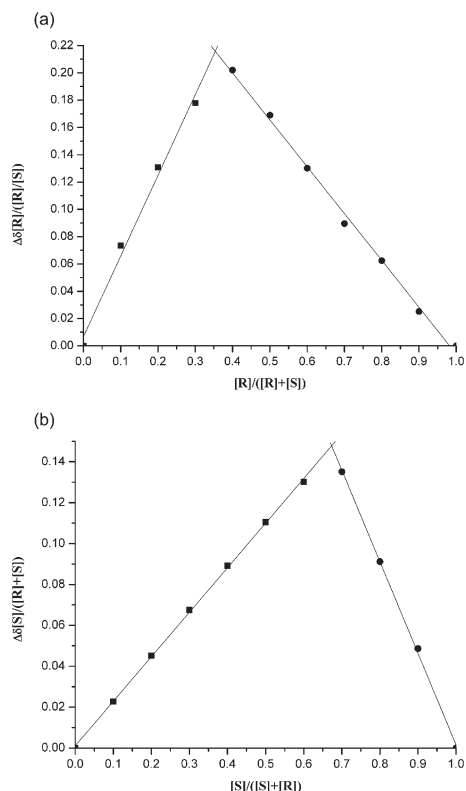


Fig. 2 Job's plots in function of (a) the receptor and (b) the substrate, for the case of terephthalate as the substrate anion.

Table 2 Association constants of receptor $(\text{H}_6\text{Me}_2[28]\text{py}_2\text{N}_6)^{6+}$ with different anions, at 25°C in $\text{DMSO}-d_6$ ^a

Substrate	$\log K_1$	$\log \beta_2$	$\log K_2$
Oxalate	—	5.68(3)	—
Malonate	—	5.96(4)	—
Succinate	3.45(6)	6.15(7)	2.69(7)
Glutarate	3.28(6)	5.87(5)	2.59(5)
Adipate	3.51(6)	6.40(5)	2.89(5)
Benzoate	—	5.94(4)	—
3-Nitrobenzoate	2.86(2)	—	—
4-Nitrobenzoate	2.99(2)	—	—
Phthalate	3.33(5)	6.11(4)	2.78(4)
Isophthalate	3.69(9)	—	—
Terephthalate	3.20(4)	5.35(2)	2.15(2)
4,4'-Dibenzoate	—	5.51(3)	—

^aErrors in K are the standard deviations given directly by the program HypNMR²⁶ by fitting of experimental points from about 30 NMR signals measured.

type of binding, as expected because all the interactions occur between carboxylate groups of the substrate and ammonium ions of the receptor. These results also indicate a co-operative effect, as the binding of the first guest molecule partially neutralizes the positive charge of the central secondary amine decreasing the electrostatic repulsion within the receptor-molecule allowing it to adopt an appropriate conformation for the binding of the second substrate anion. This co-operative effect seems to be higher for oxalate, malonate, benzoate and 4,4'-dibenzoate for which it was not possible to distinguish the first from the second constants.

The behaviour of benzoate is striking. Indeed this monoanion forms two species with the receptor, with constants of comparable magnitude to those found for the dicarboxylate anions. Furthermore, the shift of the resonances presents patterns similar to those observed for the dicarboxylate anions suggesting that the first anion interacts with the central ammonium of the receptor and the second one will share the interaction with ammonium centres contiguous to the pyridine. However for the two other monocarboxylates studied, 3-nitro and 4-nitrobenzoate anions, it was only possible to determine their first association constants, which are the lowest constants in Table 2. In fact these anions are less basic than benzoate and it seems that the nitro group is not co-ordinated by hydrogen bonds to the ammonium centres of the receptor.

The fact that two association constants have been determined for the binding of dicarboxylate substrates to $(\text{H}_6\text{Me}_2[28]\text{py}_2\text{N}_6)^{6+}$ and the similarity of the values for the different anions, clearly suggests that the substrate molecules are not included within the cavity provided by the macrocycle. Each substrate may interact with different sites of the same receptor-molecule, or alternatively bind to more than one receptor-molecule.

The use of a polar solvent, such as $\text{DMSO}-d_6$, does not favour hydrogen bonding and electrostatic interactions between the receptor and the substrate, however the insolubility of some of the anionic substrates in less polar solvents required this choice of solvent. The method used for the determination of the association constants, comprising the addition of aliquots of substrate solutions to the receptor, favours intermolecular interactions between the receptor and several substrates.

The ^1H NMR method used, although less appropriate for accurate determinations of equilibrium constants for more complex systems, has the advantage of giving more structural information. Indeed, it was possible to establish that the central ammonium ($-\text{HNCH}_3^+$) sites are the most available for the first carboxylate binding, and the ammonium centres adjacent to the pyridine ring are the favourite sites for the binding of the second substrate. This feature suggests that in the conformation adopted by the macrocycle in DMSO the H-atoms of the central ammonium sites are exposed in such a way as to easily form hydrogen-bonding interactions with the substrate.

X-Ray determination: crystal structures of $[\text{H}_6\text{Me}_2[28]\text{py}_2\text{N}_6]^{6+}$ with (terephthalate) $^{2-}$ and (4,4'-dibenzoate) $^{2-}$ †

X-Ray single crystal diffraction studies establish the existence of molecular aggregates between the $[\text{H}_6\text{Me}_2[28]\text{py}_2\text{N}_6]^{6+}$ cation and the anions (terephthalate) $^{2-}$ **1** and (4,4'-dibenzoate) $^{2-}$ **2**. Both compounds contain asymmetric units composed of one-half of the macrocyclic cation, one PF_6^- anion and two water molecules. The asymmetric unit content is completed by two-half independent molecules of (terephthalate) $^{2-}$ in **1** and one entire molecule of (dibenzoate) $^{2-}$ in **2**. Thus, both aggregate compounds have the molecular formula $(\text{H}_6\text{Me}_2[28]\text{py}_2\text{N}_6) \cdot (\text{substrate})_2 \cdot (\text{PF}_6)_2 \cdot 4\text{H}_2\text{O}$ (substrate = terephthalate $^{2-}$ or 4,4'-dibenzoate $^{2-}$), which is consistent with the protonation of all six sp^3 nitrogen centres of the macrocycle. Indeed as mentioned

† CCDC reference numbers 238466 and 238467. See <http://www.rsc.org/suppdata/ob/b4/b412059k/> for crystallographic data in .cif or other electronic format.

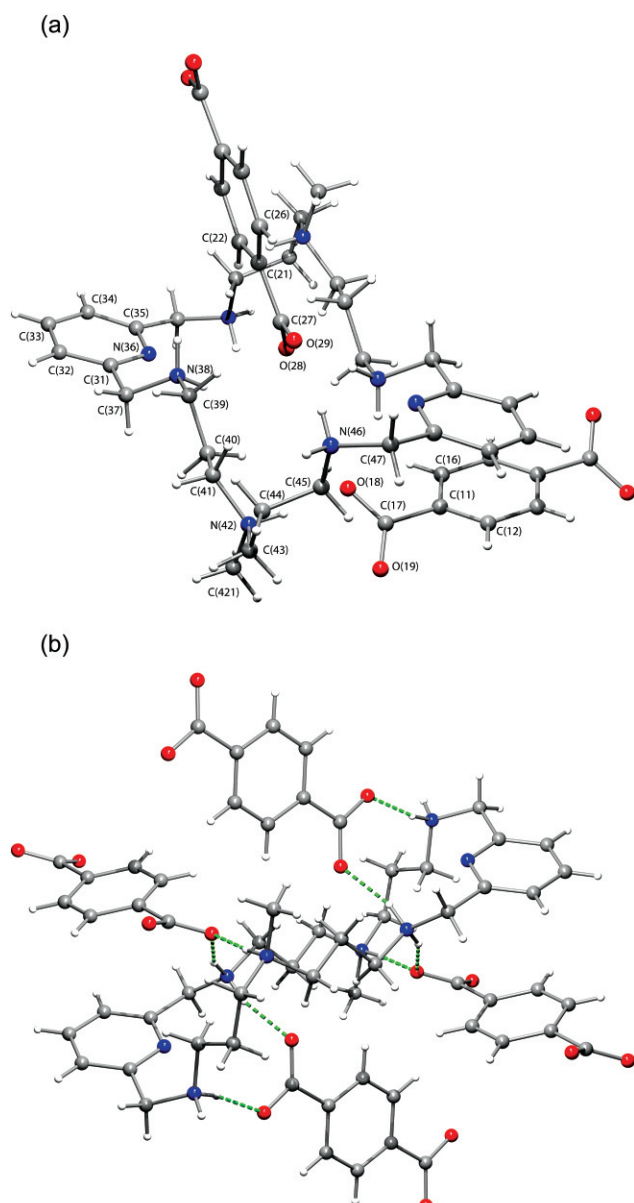


Fig. 3 Structure of the supramolecular aggregate $[\text{H}_6\text{Me}_2[28]\text{py}_2\text{N}_6]^{6+} \cdot (\text{terephthalate})^{2-}$ **1** (a) Molecular diagram showing the overall disposition of the macrocyclic receptor and the anions in the R:2S ratio. Labelling scheme of the atoms generated by symmetry is not shown for clarity. The symmetry operations to generate equivalent atoms are: $-x + 1, -y + 1, -z$ for those from the macrocyclic framework; $-x + 2, -y + 2, -z$ for the first terephthalate [O(18) to C(16)] and $-x, -y + 1, -z$ for the second one [O(28) to C(26)] respectively); (b) the $[\text{H}_6\text{Me}_2[28]\text{py}_2\text{N}_6]^{6+}$ cation binding *via* hydrogen bonds to four surrounding terephthalate $^{2-}$ anions.

above the $[\text{H}_6\text{Me}_2[28]\text{py}_2\text{N}_6]^{6+}$ species was titrated with the diprotonated substrate. Molecular diagrams showing the overall structures of the organic substrates and the macrocyclic receptor together with the labelling scheme adopted are presented in Figs. 3 and 4 for **1** and **2**, respectively. The bond distances and angles found for the substrates and receptor are within the expected values. In both compounds the macrocycle exhibits a centrosymmetric conformation of ladder type shape, but with significant differences in the endocyclic torsion angles, see Table 3. This is consistent with the flexibility of the macrocyclic framework derived from the large dimensions of $\text{Me}_2[28]\text{py}_2\text{N}_6$. Additionally in these two compounds, $[\text{H}_6\text{Me}_2[28]\text{py}_2\text{N}_6]^{6+}$ is involved in an extensive network of hydrogen bonds which have necessarily a different pattern: **1** and **2** crystallise in space groups $P\bar{1}$ and $P2_1/c$, respectively. In other words the crystal packing, particularly the hydrogen bonding interactions, determine the conformation of the protonated macrocycle.

The dimensions of hydrogen bonds found for compounds **1** and **2** are listed in Table 4 and show that the receptor, the organic

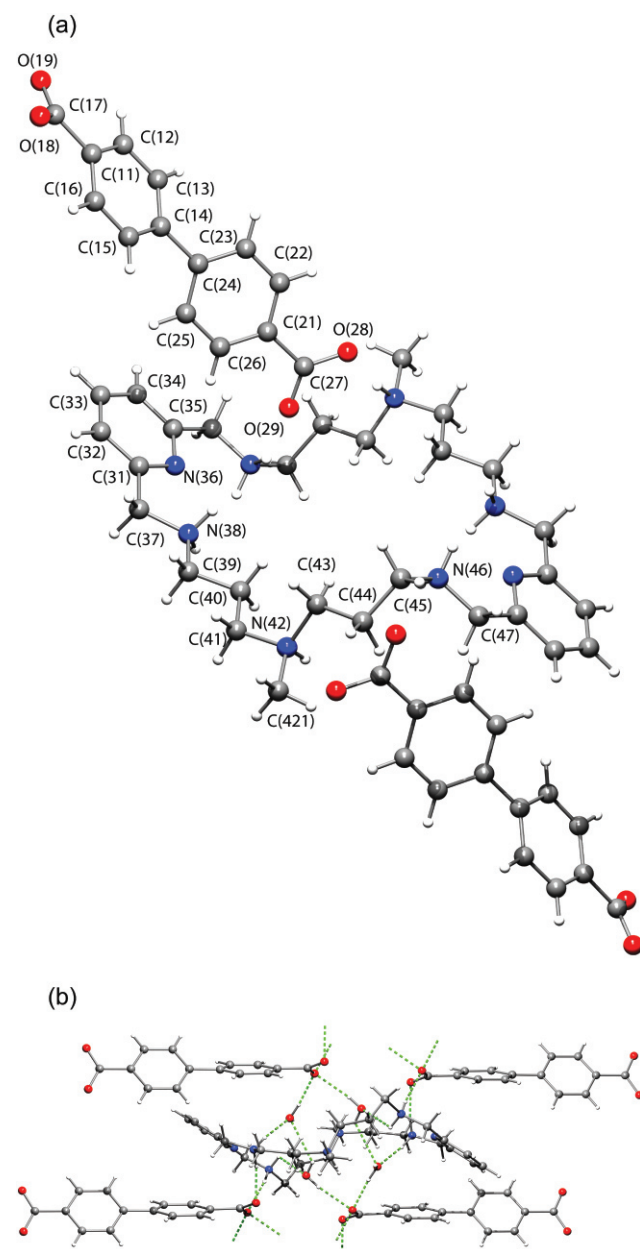


Fig. 4 Structure of the supramolecular aggregate $[\text{H}_6\text{Me}_2[28]\text{py}_2\text{N}_6]^{6+} \cdot (4,4'\text{-dibenzoate})^{2-}$ **2**: (a) Molecular diagram showing the overall disposition of the macrocyclic receptor and the anions in the R:2S ratio. The unlabelled atoms are generated by the symmetry operation $[-x + 2, -y, -z]$ and its labelling scheme is omitted for clarity; (b) a $[\text{H}_6\text{Me}_2[28]\text{py}_2\text{N}_6]^{6+}$ entire molecule binding *via* hydrogen bonds to four surrounding 4,4'-dibenzoate $^{2-}$ anions and to four water molecules.

Table 3 Endocyclic torsion angles (°) for compounds **1** and **2**

Compound	1	2
N(36)–C(35)–C(37)–N(38)	39.2(6)	20.5(8)
C(35)–C(37)–N(38)–C(39)	166.4(4)	171.8(5)
C(37)–N(38)–C(39)–C(40)	77.1(5)	–169.5(6)
N(38)–C(39)–C(40)–C(41)	–173.2(4)	–179.8(5)
C(39)–C(40)–C(41)–N(42)	–160.0(5)	–170.8(5)
C(40)–C(41)–N(42)–C(43)	–174.4(4)	62.1(7)
C(41)–N(42)–C(43)–C(44)	–51.0(6)	165.2(5)
N(42)–C(43)–C(44)–C(45)	–66.6(7)	159.8(5)
C(43)–C(44)–C(45)–N(46)	178.4(5)	–88.8(7)
C(44)–C(45)–N(46)–C(47)	146.6(5)	–77.9(7)
C(45)–N(46)–C(47)–C(31*) ^a	56.5(6)	–177.3(5)

^a* is symmetry operation $-x + 1$, $-y + 1$, $-z$ for **1** and $-x + 2$, $-y$, $-z$ for **2**.

substrates (terephthalate²⁻ and 4,4'-dibenzoate²⁻) and solvent water molecules are assembled into a 3-D network of N–H...O and O–H...O hydrogen bonding interactions. In addition, for compound **1**, several short intermolecular contacts between N–H groups and the fluorine atoms are also found but they are not included in the Table 4 due to the disorder exhibited by the PF₆⁻ counter-ion.

On the other hand Figs. 3(b) and 4(b) clearly show that the macrocycle binds the substrates *via* N–H...O hydrogen bonds but these substrates are positioned outside of the macrocyclic cavity. This structural feature is somewhat unexpected given the flexibility and the large dimensions of the macrocycle together with the protonation of six nitrogen donor-binding sites. However the macrocycle is not pre-organised for the entry of these two substrates into its cavity, and consequently the molecular recognition mechanism occurs outside the macrocyclic cavity *via* N–H...O hydrogen bonds but without the formation of an inclusion complex.

Different features illustrating the crystal building of **1** are presented in Fig. 5 in three frames. The [H₆Me₂[28]py₂N₆]⁶⁺ receptors (see Fig. 5a) are bridged by the second independent terephthalate²⁻ substrate *via* hydrogen bonds between the N–H groups adjacent to the pyridine rings and the two oxygen atoms from two carboxylate groups (four C=O...H–N distances, two of 1.81 Å and two of 1.86 Å) with the formation of 1-D chains. Subsequently, adjacent chains are bridged by one of the independent water molecules thorough the hydrogen bonds involving one oxygen atom of carboxylate groups (O–H...O = 2.05(11) Å) and one N–H group from the macrocycle (2.01 Å) leading to the formation of layers (see Fig. 5b), which are further connected by the carboxylate of the first independent terephthalate (four C=O...H–N distances, two of 1.80 Å and two of 1.96 Å) giving

the final 3-D supramolecular architecture. These last two hydrogen bonds involve only one independent oxygen atom O(18) from a carboxylate group together with the N–H groups from different macrocyclic linkages: the H(38) bonded to N–Me group [$1 - x$, $-y$, $-z$] and the N(42) adjacent to the pyridine ring. This fact leads to the twisting of the first carboxylate, relative to the aromatic ring by 34.4(4)°. By contrast in the second terephthalate substrate the two carboxylate groups and the aromatic ring are almost coplanar and the angle between their planes is only 8.8(4)°. The remaining oxygen atom from the carboxylate forms hydrogen bonds with the first solvation water molecule (O–H...O of 2.24(11) Å). Fig. 5(c) shows a picture of the lattice in which is emphasised the relative orientation of the terephthalate substrates and the interstitial sites of the 3-D network hydrogen bonds occupied by PF₆⁻ anions.

The crystal building features of **2** are presented in Fig. 6. The two independent water molecules interact *via* a H...O–H hydrogen bond [2.50(7) Å] forming a dimer. As shown in Fig. 6(a), each receptor macrocycle encapsulates two water dimers through hydrogen bonds between the N–H groups adjacent to the pyridine rings and the oxygen atoms from two independent water molecules (two water bridges with H–N...O distances of 2.38 Å and two of 1.74 Å). Subsequently the 4,4'-dibenzoate²⁻ substrate bridges the [H₆Me₂[28]py₂N₆]⁶⁺ cations giving rise to a 3-D network of N–H...O hydrogen bonds [see Fig. 6(b)]. The oxygen atoms from the carboxylate group bonded to C17 are connected to the remaining N–H groups adjacent to the pyridine rings (two N–H...O distances of 1.90 and 1.85 Å) while the two oxygen atoms of the second one binds the N–H group adjacent to the pyridine ring (H–N...O of 2.06 Å) and the consecutive N–H protonated site of the same macrocyclic linkage (H–N...O distance of 1.72 Å); this hydrogen also interacts with water molecule O(200). In order to establish this supramolecular architecture, the 4,4'-dibenzoate²⁻ is twisted with an angle between the two aromatic rings of 44.0(9)°. The hydrogen bonding pattern is completed with O–H...O hydrogen bonds involving the water molecule O(100) with the oxygen atom O(19) from a carboxylate group [2.05(4) Å]. In Fig. 6c is shown the [H₆Me₂[28]py₂N₆]⁶⁺ cations forming open channels which are occupied by water molecules. The PF₆⁻ anions are located between these channels.

In conclusion, the organic substrates in both compounds work as the pillars of the supramolecular architectures described. The building block role is reserved for aggregates with a stoichiometry R₂S₂ and with the substrates located outside the macrocyclic cavity, such as was recently found in the association between a related 26-membered hexaazamacrocyclic and oxalate anion.¹³

Conclusions

The binding ability of the receptor [H₆Me₂[28]py₂N₆]⁶⁺ was evaluated towards a wide range of aliphatic and aromatic

Table 4 Dimensions of the hydrogen bonds in the supramolecular aggregates (H₆Me₂[28]py₂N₆)-(substrate)₂(PF₆)₂·4H₂O **1** and **2**

Substrate	H...A/Å	D...A/Å	D...H...A/°
Terephthalate²⁻ 1			
N(46)–H(46A)···O(29)	1.81	2.693(7)	167
N(46)–H(46B)···O(200) [$1 - x$, $2 - y$, $1 - z$]	2.01	2.820(9)	150
N(42)–H(42)···O(18)	1.80	2.706(6)	174
N(38)–H(38A)···O(28) [$1 - x$, $1 - y$, $-z$]	1.86	2.733(6)	164
N(38)–H(38B)···O(18) [$1 - x$, $-y$, $-z$]	1.96	2.811(6)	157
O(100)–H(101)···O(19) [$-1 + x$, $-1 + y$, z]	2.24(11)	2.914(12)	138(11)
O(200)–H(202)···O(29)	2.05(11)	2.745(11)	141(11)
4,4'-Dibenzoate²⁻ 2			
N(38)–H(38A)···O(100)	1.74	2.637(8)	172
N(38)–H(38B)···O(18) [$1 + x$, $1/2 - y$, $-1/2 + z$]	1.85	2.738(6)	167
N(42)–H(42)···O(29)	1.72	2.625(6)	170
N(46)–H(46B)···O(19) [$1 + x$, $1/2 - y$, $-1/2 + z$]	1.90	2.754(7)	157
N(46)–H(46A)···O(28)	2.06	2.856(6)	147
N(46)–H(46A)···O(200) [$1 + x$, $1/2 - y$, $-1/2 + z$]	2.38	2.825(10)	110
O(100)–H(101)···O(19) [x , $1/2 - y$, $-1/2 + z$]	1.85(3)	2.671(7)	172(6)
O(100)–H(102)···O(28)	1.88(4)	2.683(7)	164(8)
O(200)–H(201)···O(100) [$-1 + x$, $1/2 - y$, $1/2 + z$]	2.50(7)	3.091(10)	130(7)
O(200)–H(202)···O(19) [$1 - x$, $1 - y$, $1 - z$]	2.04(4)	2.855(7)	171(5)

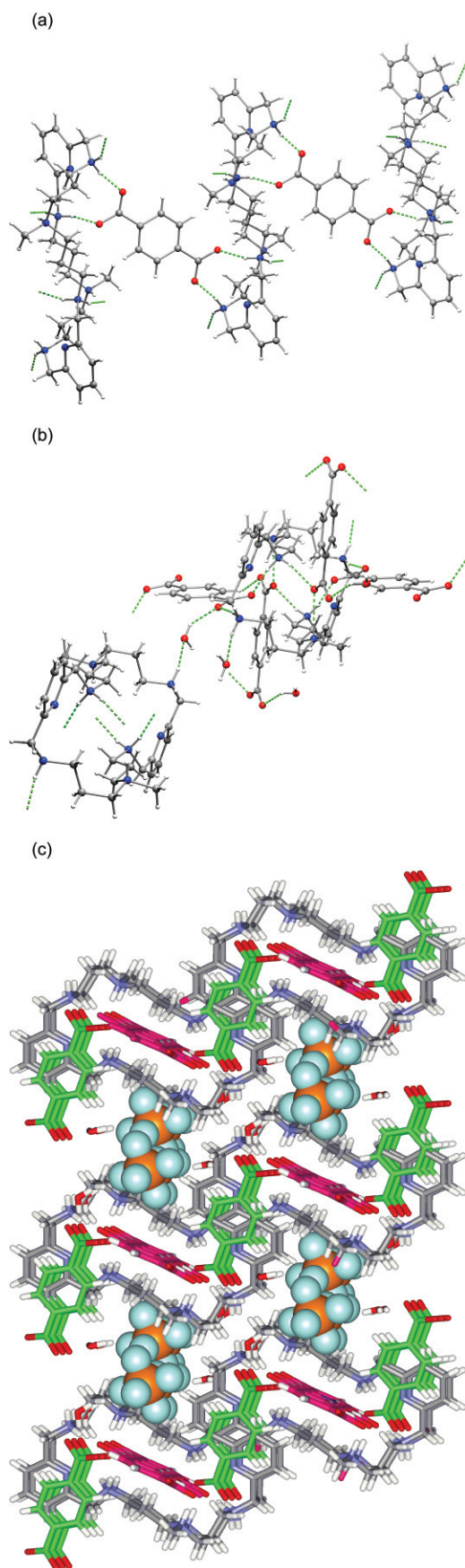


Fig. 5 Crystal building of $(\text{H}_6\text{Me}_2[28]\text{py}_2\text{N}_6)\text{-(terephthalate)}_2\text{-(PF}_6)_2\cdot 4\text{H}_2\text{O}$. (a) 1-D dimensional chain resulting from the interaction *via* hydrogen bonds of $(\text{H}_6\text{Me}_2[28]\text{py}_2\text{N}_6)^{6+}$ and the first independent terephthalate²⁻ anion. (b) 3-D network hydrogen bonds after inclusion of the second independent terephthalate²⁻ anion and solvent water molecules; (c) crystal packing diagram showing the disposition of the terephthalate²⁻ and PF_6^- anions. Only the octahedrally-disposed fluorine atoms with the major occupancy are shown.

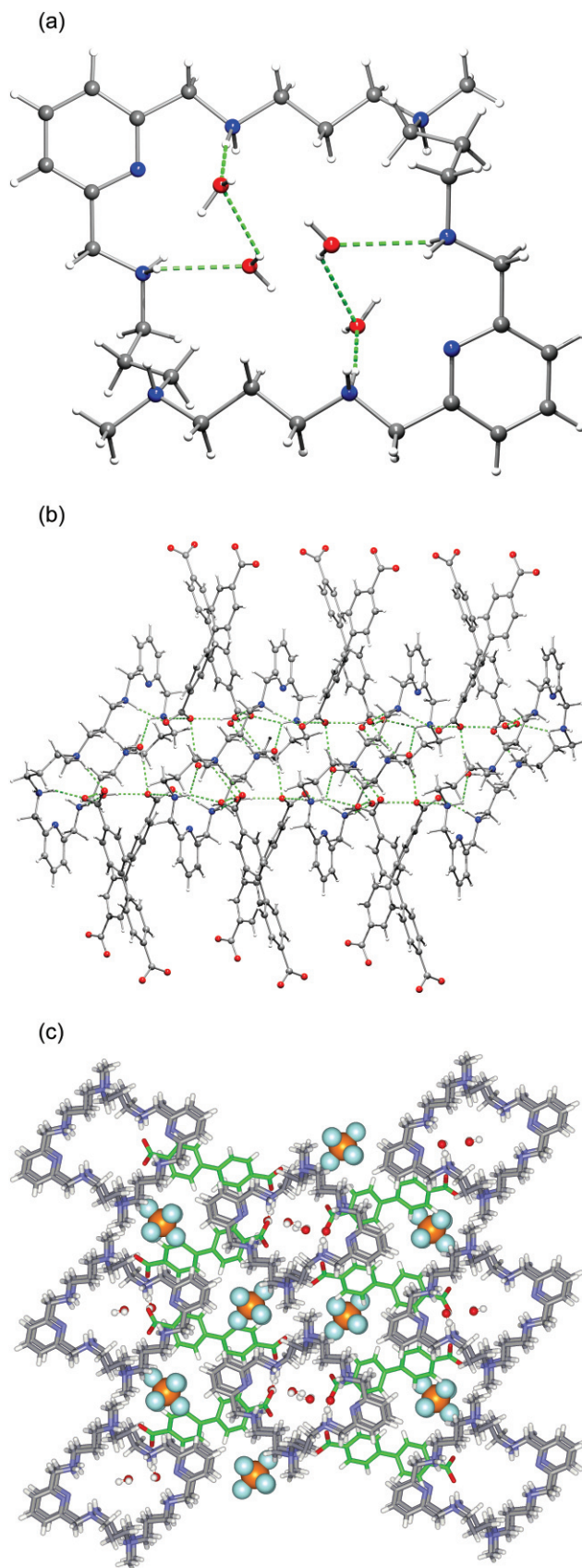


Fig. 6 Crystal building of $(\text{H}_6\text{Me}_2[28]\text{py}_2\text{N}_6)\text{-(4,4'-dibenzoate)}_2\text{-(PF}_6)_2\cdot 4\text{H}_2\text{O}$. (a) Four water solvent molecules are encapsulated in the $(\text{H}_6\text{Me}_2[28]\text{py}_2\text{N}_6)^{6+}$ macrocyclic cavity; (b) 3-D network hydrogen bonds derived from the interaction between $(\text{H}_6\text{Me}_2[28]\text{py}_2\text{N}_6)^{6+}$, 4,4'-dibenzoate anions and solvent water molecules; (c) crystal packing diagram showing open channels formed by the receptor molecules filled by the water molecules. The PF_6^- anions occupy the remaining interstitial space available in the lattice.

carboxylate anions having different sizes, shapes and flexibility. The binding studies were carried out by ^1H NMR titration techniques in solution ($\text{DMSO-}d_6$) and by single crystal X-ray crystallography in the solid state. The $^1\text{H-NMR}$ binding studies (see Tables 1 and 2) have shown that each receptor $[\text{H}_6\text{Me}_2[28]\text{py}_2\text{N}_6]^{6+}$ assembles two molecules of all substrates. The unique exceptions are the monocarboxylate 3-nitro- and 4-nitrobenzoate anions, for which only the first association constant was determined, suggesting that only $\text{H}_6\text{Me}_2[28]\text{py}_2\text{N}_6:(\text{substrate})$ species are formed. Indeed the X-ray single crystal structures of $[\text{H}_6\text{Me}_2[28]\text{py}_2\text{N}_6]^{6+}$ cation with the anions (terephthalate) $^{2-}$ **1** and (4,4'-dibenzoate) $^{2-}$ **2** have revealed that in the solid state the molecular assembly of these species yields compounds with the general formula $(\text{H}_6\text{Me}_2[28]\text{py}_2\text{N}_6)(\text{substrate})_2(\text{PF}_6)_2 \cdot 4\text{H}_2\text{O}$. In both crystal structures the $[\text{H}_6\text{Me}_2[28]\text{py}_2\text{N}_6]^{6+}$ cations, the substrate anions and water molecules are connected into extensive 3-D networks of hydrogen bonds. The (terephthalate) $^{2-}$ **1** and (4,4'-dibenzoate) $^{2-}$ **2** anions are the pillars of the corresponding molecular assembly. Indeed no inclusion compound $(\text{H}_6\text{Me}_2[28]\text{py}_2\text{N}_6)(\text{substrate})^{2-}$ is formed and the structures reported here represent two more examples in which the molecular recognition of the substrate occurs outside the receptor macrocyclic cavity.

Experimental

Microanalyses were carried out by the ITQB Microanalytical Service. The ^1H and ^{13}C NMR spectra were determined on a Bruker CXP 300 spectrometer. FAB mass spectra were recorded on an AutoSpecEQ mass spectrometer at the University of Aveiro.

Reagents

$\text{Me}_2[28]\text{py}_2\text{N}_6$ was synthesized by a previously described procedure,²³ and used in its hexaprotonated form, $(\text{H}_6\text{Me}_2[28]\text{py}_2\text{N}_6)(\text{PF}_6)_6$ by reaction with hexafluorophosphoric acid (60 wt% in water) from Aldrich. The anions were prepared from the commercially available acids by reaction with tetramethylammonium hydroxide (25 wt% in water solution from Aldrich). $(\text{CD}_3)_2\text{SO}$ ($\text{DMSO-}d_6$) was purchased from Aldrich and used as freshly opened ampoules. The references used for the ^1H and ^{13}C NMR measurements in $\text{DMSO-}d_6$ were 3-(trimethylsilyl)propanoic acid- d_4 -sodium salt and 1,4-dioxane, respectively.

Preparation of $(\text{H}_6\text{Me}_2[28]\text{py}_2\text{N}_6)(\text{PF}_6)_6$

$\text{Me}_2[28]\text{py}_2\text{N}_6$ (0.15 g) was dissolved in water (10 mL) and HPF_6 (60%) was added until pH 4. Upon partial evaporation of the solvent a fine white precipitate was formed, which was washed with ethanol and dried under vacuum. Yield: 85%. $(\text{H}_6\text{Me}_2[28]\text{py}_2\text{N}_6)(\text{PF}_6)_6$: ^1H NMR ($\text{DMSO-}d_6$): δ 2.198 (8 H, q, $\text{NCH}_2\text{CH}_2\text{CH}_2\text{N}$), 2.835 (6 H, s, NCH_3), 3.135 (8 H, t, $\text{NCH}_2\text{CH}_2\text{CH}_2\text{N}$), 3.208 (8 H, t, $\text{NCH}_2\text{CH}_2\text{CH}_2\text{N}$), 4.451 (8 H, s, pyCH_2N), 7.551 (4 H, d, py) and 8.030 (2 H, t, py). ^{13}C NMR ($\text{DMSO-}d_6$): δ 21.7 ($\text{NCH}_2\text{CH}_2\text{CH}_2\text{N}$), 44.6 ($\text{NCH}_2\text{CH}_2\text{CH}_2\text{N}$), 49.9 (NCH_3), 51.5 ($\text{NCH}_2\text{CH}_2\text{CH}_2\text{N}$), 66.4 (pyCH_2N), 122.5 (py), 138.7 (py) and 151.4 (py). Found: C, 24.63; H, 3.79; N, 8.13%. Calc. for $\text{C}_{28}\text{H}_{54}\text{F}_6\text{N}_8\text{P}_6$: C, 24.44; H, 3.95; N, 8.14%. FAB MS: m/z 497 [HL^+], 643 [$\text{H}_2\text{L}^{2+} + \text{PF}_6^-$], 789 [$\text{H}_3\text{L}^{3+} + 2\text{PF}_6^-$], 935 [$\text{H}_4\text{L}^{4+} + 3\text{PF}_6^-$], 1082 [$\text{H}_5\text{L}^{5+} + 4\text{PF}_6^-$], 1227 [$\text{H}_6\text{L}^{6+} + 5\text{PF}_6^-$], 1376 [$\text{H}_7\text{L}^{7+} + 6\text{PF}_6^-$].

Preparation of tetramethylammonium carboxylate salts

To a stirred solution of the carboxylic acid (10.0 mmol) in water (20 mL) was added 1.0 or 2.0 equiv. (for the mono or dicarboxylic acids, respectively) of a solution of tetramethylammonium hydroxide (1.0 M) in water. The solvent was then evaporated and the salts were recrystallized from acetone and dried under vacuum.

Preparation of single crystals

Crystals of **1** and **2** suitable for X-ray crystallographic studies were obtained using the following procedure: an aqueous solution

of the salt $(\text{Me}_4\text{N})_2$ -terephthalate or $(\text{Me}_4\text{N})_2$ -(4,4'-dibenzoate) (0.044 mmol, 0.029 g or 0.082 mmol, 0.0039 g, respectively) was added to a stirred solution of $(\text{H}_6\text{Me}_2[28]\text{py}_2\text{N}_6)(\text{PF}_6)_6$ (0.02 mmol, 0.029 g) in water (10.0 mL). The mixture was stirred for 2 h, and then the solvent was removed under vacuum and taken up in methanol. The precipitate formed was filtered off and recrystallized from $\text{H}_2\text{O-CH}_3\text{OH}$ (1 : 1). White crystals were formed in five days by slow evaporation of the solvent at room temperature.

^1H NMR titrations and determination of the association constants

To the solution of the compound $(\text{H}_6\text{Me}_2[28]\text{py}_2\text{N}_6)(\text{PF}_6)_6$ (0.6 mL, 2–3 mM) in $\text{DMSO-}d_6$ were added portions of 0.01 mL of the TMA salt of each carboxylate (20–30 mM) dissolved also in $\text{DMSO-}d_6$ at 300 K. The initial ^1H NMR was recorded with no anion present, and then aliquots of anion salt solutions were added using a Hamilton syringe (Microliter 700 series of 25 μL) or a micropipette of 250 μL (EDP-2). About 30 to 40 additions were necessary for each titration until no further change in the chemical shift was observed, except when isophthalate and terephthalate were used, for which precipitation occurred. A Bruker CXP 300 spectrometer was used to perform the ^1H NMR spectra, and each solution was left for 15 to 30 min to stabilize. No effort was made to maintain a constant ionic strength to avoid competition from other anions, but care was taken to avoid water absorption from the atmosphere.

Changes in the chemical shift of all the protons were recorded, except for proton H_d that is the most difficult to follow. The association constants of the various species formed in solution were determined from the experimental data corresponding to the titration of solutions of the receptor with different anions using HypNMR,²⁶ which requires as input the concentration of each component and the observed chemical shift. The fitting procedure yielded the binding constant and chemical shift for each $\text{R}:\text{S}_i$ species. Initial calculations provided overall stability constants, $\beta_{\text{R},\text{S}}$ values, $\beta_{\text{R},\text{S}} = [\text{R}_i\text{S}_i]/[\text{R}][\text{S}]^i$. RS and RS_2 species were found in most cases. Differences between the values of $\log \beta_{\text{RS}}$ and $\log \beta_{\text{RS}_2}$ provide the stepwise reaction constants. The errors quoted are the standard deviations of the overall stability constants given directly by the program from the input data, which include the experimental points for all resonances of the titration curves. The standard deviations of the stepwise constants, shown in Table 2, were determined by the normal propagation rules.

Job's plots

Stock solution for the host (conc. from 2.13 to 7.85 mM) and for the tetramethylammonium salts of guests (in the same concentrations) in $\text{DMSO-}d_6$ were prepared. Ten NMR tubes were filled with 500 μL solutions of the host and guest in the following volume ratios: 50:450, 100:400, 150:350, 200:300, 250:250, 300:200, 350:150, 400:100, 450:50, 500:0. ^1H NMR spectra were recorded and the concentration of the complex ($[\text{C}]$) for each solution was determined from the equation, $[\text{C}] = [\text{R}]_0 \times (\delta_{\text{obs}} - \delta_{\text{R}}) / (\delta_{\text{max}} - \delta_{\text{R}})$, where $[\text{R}]_0$ is the total receptor concentration, δ_{obs} is the observed chemical shift, δ_{R} is the chemical shift of the free receptor, and δ_{max} is the chemical shift of the complex. Because $(\delta_{\text{max}} - \delta_{\text{R}})$ is a constant, the concentration of the complex is proportional to $\Delta\delta \times [\text{R}]_0$ [being $\Delta\delta = (\delta_{\text{obs}} - \delta_{\text{R}})$]. Plots of $\Delta\delta X_{\text{R}}$ as a function of X_{R} (where X_{R} is the molar fraction of the receptor) and of $\Delta\delta X_{\text{S}}$ as a function of X_{S} (where X_{S} is the molar fraction of the substrate) were performed for the cases of malonate, glutarate and terephthalate.^{24,25}

Crystallography†

Suitable crystals for X-ray diffraction analysis of molecular aggregates **1** and **2** were obtained at room temperature from an aqueous solution of $[\text{H}_6\text{Me}_2[28]\text{py}_2\text{N}_6](\text{PF}_6)_6$ and (terephthalate) $^{2-}$ **1**, and (4,4'-dibenzoate) $^{2-}$ **2**. The diffusion method with CH_3OH

Table 5 Room temperature crystal data and pertinent refinement details for compounds **1** and **2**

	1	2
Empirical formula	C ₄₄ H ₇₀ F ₁₂ N ₈ O ₁₂ P ₂	C ₅₆ H ₇₈ F ₁₂ N ₈ O ₁₂ P ₂
Molecular formula	[C ₂₈ H ₅₄ N ₈] ₂ (C ₈ H ₄ O ₄) ₂ (PF ₆) ₂ ·4(H ₂ O)	[C ₂₈ H ₅₄ N ₈] ₂ (C ₁₄ H ₈ O ₄) ₂ (PF ₆) ₂ ·4(H ₂ O)
M _w	1193.02	1345.20
Crystal system	Triclinic	Monoclinic
Space group	<i>P</i> $\bar{1}$	<i>P</i> 2 ₁ / <i>c</i>
<i>a</i> /Å	10.818(11)	8.040(10)
<i>b</i> /Å	11.701(13)	28.570(29)
<i>c</i> /Å	12.827(13)	13.420(15)
<i>a</i> °	105.10(1)	(90.0)
<i>β</i> °	101.25(1)	93.41(1)
<i>γ</i> °	115.44(1)	(90.0)
<i>V</i> /Å ³	1324.9	3077.2
<i>Z</i>	1	2
<i>D</i> _c /Mg m ⁻³	1.495	1.452
<i>μ</i> /mm ⁻¹	0.191	0.174
Reflections collected	7479	11010
Unique reflections, [<i>R</i> _{int}]	4442, [0.0359]	4420 [0.1446]
Final <i>R</i> indices		
<i>R</i> ₁ , <i>wR</i> ₂ [<i>I</i> > 2σ <i>I</i>]	0.1101; 0.2736 [3600]	0.0956; 0.1806 [2611]
<i>R</i> ₁ , <i>wR</i> ₂ (all data)	0.1278; 0.2874	0.1522; 0.2043

as the diffusing solvent was used. The pertinent crystallographic data are given in Table 5. X-Ray data were collected at room temperature on a MAR research plate system using graphite monochromatised Mo-K α radiation ($\lambda = 0.71073$ Å) at Reading University. The crystals were positioned at 70 mm from the image plate. 95 frames were taken at 2° intervals using an appropriate counting time. Data analysis was performed with XDS program.²⁷ Intensities of compound **1** were not corrected for absorption effects while an empirical absorption correction was applied to the intensities of the compound **2** using the DIFABS program.²⁸

Both structures were solved by direct methods and by subsequent difference Fourier syntheses and refined by full matrix least squares on *F*² using the SHELX-97 system programs.²⁹ The earliest difference Fourier maps calculated for **1** revealed that the fluorine atoms of the PF₆⁻ anion were disordered. Two sets of octahedral fluorine atoms were considered and their occupancies with 1 - *x* and *x* respectively, *x* being equal to 0.62(1). The P-F and F...F distances were constrained in order to give an ideal octahedral geometry. Anisotropic thermal parameters were used for all non-hydrogen atoms except for fluorine atoms of the PF₆⁻ counter ion of **1**, which were refined with individual isotropic temperature factors. The hydrogen atoms bonded to carbon and nitrogen atoms were included in calculated positions. The hydrogen atoms of the water molecules were located from difference Fourier maps and refined with O-H distances and H-O-H angles constrained to 0.82 Å and 104.5°, respectively. The thermal movement of hydrogen atoms was described using isotropic parameters equivalent to 1.2 times those of the atom to which were attached, except the hydrogen atoms of water molecules in **2**, which were refined with individual isotropic thermal parameters. The residual electronic density ranging from 1.060 to -0.834 eÅ⁻³ for **1** and 0.587 to -0.287 eÅ⁻³ for **2**, were within expected values.

The ORTEP diagrams were drawn with graphical package software PLATON³⁰ while the remaining X-ray diagrams presented were performed with WEBLAB VIEWER.³¹

Acknowledgements

The authors acknowledge the financial support from Fundação para a Ciência e Tecnologia (FCT) and POCTI, with co-participation of the European Community fund FEDER (Project n. POCTI/1999/QUIM/35396).

References

- 1 *Supramolecular Chemistry of Anions*, ed. A. Bianchi, K. Bowman-James and E. Garcia-España, Wiley-VCH, New York, 1997.
- 2 C. A. Ilioudis and J. W. Steed, *J. Supramol. Chem.*, 2001, **1**, 165.

- 3 R. J. Fitzmaurice, G. M. Kyne, D. Douheret and J. D. Kilburn, *J. Chem. Soc., Perkin Trans. 1*, 2002, 841.
- 4 J. M. Llinares, D. Powell and K. Bowman-James, *Coord. Chem. Rev.*, 2003, **240**, 57.
- 5 C. R. Bondy and S. J. Loeb, *Coord. Chem. Rev.*, 2003, **240**, 77.
- 6 P. A. Gale, *Coord. Chem. Rev.*, 2000, **199**, 181; P. A. Gale, *Coord. Chem. Rev.*, 2001, **213**, 79; P. A. Gale, *Coord. Chem. Rev.*, 2003, **240**, 191.
- 7 B. Dietrich, M. W. Hosseini, J. M. Lehn and R. B. Sessions, *J. Am. Chem. Soc.*, 1981, **103**, 1282.
- 8 E. Kimura, A. Sakonaka, T. Yatsunami and M. Kodama, *J. Am. Chem. Soc.*, 1981, **103**, 3041.
- 9 (a) F. H. Allen, *Acta Crystallogr., Sect. B: Struct. Sci.*, 2002, **58**, 380; (b) I. J. Bruno, J. C. Cole, P. R. Edgington, M. Kessler, C. F. Macrae, P. McCabe, J. Pearson and R. Taylor, *Acta Crystallogr., Sect. B: Struct. Sci.*, 2002, **58**, 389.
- 10 A. Szumna and J. Jurczak, *Eur. J. Org. Chem.*, 2001, 4031.
- 11 Q. Lu, R. J. Motekaitis, J. J. Reibenspies and A. E. Martell, *Inorg. Chem.*, 1995, **34**, 4958.
- 12 J. L. Sessler, A. Andrievsky, V. Král and V. Lynch, *J. Am. Chem. Soc.*, 1997, **119**, 9385.
- 13 C. Anda, A. Llobet, A. Martell, J. Reibenspies, E. Berni and X. Solans, *Inorg. Chem.*, 2004, **43**, 2793.
- 14 S. Camiolo, P. A. Gale, M. I. Ogden, B. W. Skelton and A. H. White, *J. Chem. Soc., Perkin Trans. 2*, 2001, 1294.
- 15 J.-M. Lehn, R. Méric, J.-P. Vigneron, I. Bkouche-Waksman and C. Pascard, *J. Chem. Soc., Chem. Commun.*, 1991, 62.
- 16 A. P. Bisson, V. M. Lynch, M.-K. C. Monahan and E. V. Aslyn, *Angew. Chem., Int. Ed. Engl.*, 1997, **36**, 2340.
- 17 J. Nelson, M. Nieuwenhuyzen, I. Pál and R. M. Town, *Chem. Commun.*, 2002, 2266.
- 18 J. Nelson, M. Nieuwenhuyzen, I. Pál and R. M. Town, *Dalton Trans.*, 2004, 229.
- 19 M. H. Zaroubi, N. W. Mitzel and F. P. Schmidtchen, *Angew. Chem., Int. Ed.*, 2002, **41**, 104.
- 20 G. Müller, J. Riede and F. P. Schmidtchen, *Angew. Chem., Int. Ed. Engl.*, 1988, **27**, 1516.
- 21 F. Garcia-Tellado, S. Goswami, S.-K. Chang, S. J. Geib and A. D. Hamilton, *J. Am. Chem. Soc.*, 1990, **112**, 7393.
- 22 S. Camiolo, P. A. Gale, M. B. Hurshouse and M. E. Light, *Tetrahedron Lett.*, 2002, **43**, 6995.
- 23 C. Cruz, S. Carvalho, R. Delgado, M. G. B. Drew, V. Félix and B. J. Goodfellow, *Dalton Trans.*, 2003, 3172.
- 24 L. Sebo, F. Diederich and V. Gramlich, *Helv. Chim. Acta*, 2000, **83**, 93.
- 25 K. Hirose, *J. Inclusion Phenom. Macrocycl. Chem.*, 2001, **39**, 193.
- 26 C. Frassinetti, S. Ghelli, P. Gans, A. Sabatini, M. S. Moruzzi and A. Vacca, *Anal. Biochem.*, 1995, **231**, 374.
- 27 W. Kabsch, *J. Appl. Crystallogr.*, 1988, **21**, 916.
- 28 DIFABS program, N. Walker and D. Stuart, *Acta Crystallogr., Sect. A: Fundam. Crystallogr.*, 1983, **39**, 158.
- 29 G. M. Sheldrick, *SHELX-97*, University of Göttingen, 1997.
- 30 L. Spek, *PLATON, a Multipurpose Crystallographic Tool*, Utrecht University, Utrecht, The Netherlands, 1999.
- 31 *WEBLAB VIEWER, version 2.01*, Molecular Simulations, Inc., San Diego, 1997.